

Biomedical Materials



PAPER


In vivo evaluation of modified silk fibroin scaffolds with a mimicked microenvironment of fibronectin/decellularized pulp tissue for maxillofacial surgery

RECEIVED
14 February 2017

REVISED
25 July 2017

ACCEPTED FOR PUBLICATION
9 August 2017

PUBLISHED
22 November 2017

Thanh H Thai^{1,2} , Thongchai Nuntanarant^{2,5}, Suttatip Kamolmatyakul³ and Jirut Meesane⁴

¹ Department of Odonto-Stomatology, Can Tho Hospital of Eyes and Odonto-Stomatology, Can Tho 900000, Vietnam

² Department of Oral and Maxillofacial Surgery, Faculty of Dentistry, Prince of Songkla University, Hat Yai, Songkhla 90110, Thailand

³ Department of Preventive Dentistry, Faculty of Dentistry, Prince of Songkla University, Hat Yai, Songkhla 90110, Thailand

⁴ Institute of Biomedical Engineering, Faculty of Medicine, Prince of Songkla University, Hat Yai, Songkhla 90110, Thailand

⁵ Author to whom any correspondence should be addressed.

E-mail: drthongchai@hotmail.com

Keywords: silk fibroin, fibronectin, dental pulp, mimicked microenvironment, bone regeneration, maxillofacial surgery

Abstract

This study aimed to carry out *in vivo* testing of the formation of new bone by modified silk fibroin scaffolds with a mimicked microenvironment of fibronectin/decellularized pulp in bone defects. Silk fibroin scaffolds were fabricated into three-dimensional scaffolds before being coated with fibronectin/decellularized pulp. The coated scaffolds were implanted into rabbits. Twenty-four bicortical calvarial defects in 12 rabbits were divided randomly into two groups: non-coated and coated silk fibroin scaffolds. The rabbits were sacrificed 2, 4 and 8 weeks after operation for evaluation of new bone formation. The morphology of the scaffolds, new bone formation and histology were evaluated by scanning electron microscopy, micro-CT and hematoxylin and eosin staining, respectively. The results showed that the coated silk fibroin scaffolds had a fibrillar network and crystal particles in the porous structure. The coated silk fibroin scaffolds demonstrated the ability to induce the formation of new bone with low inflammation and high vascularization. The results indicated that the modified silk fibroin scaffolds showed suitable biological performance and promise for bone regeneration in maxillofacial surgery.

Introduction

Currently there are many patients suffering from maxillofacial disease and trauma. In severe cases, patients need to be treated with biomaterial substitutes [1]. Tissue engineering scaffolds are attractive biomaterials which show the interesting ability to induce the formation of new bone at a defect site [2]. Therefore, the design of such scaffolds is a challenge for surgeons and materials scientists. This research aimed to improve the performance of scaffolds for using in maxillofacial bone surgery.

Silk fibroin (SF) scaffolds have been used in tissue engineering for several decades [3, 4]. Because of its unique physical, mechanical and biological functionalities, SF is fabricated in porous scaffolds for bone tissue engineering [5–7]. In some studies, the porous SF scaffolds are modified to enhance their biological

functionality and these modified scaffolds are able to induce the formation of new bone [8–10]. The purpose of this study was to enhance the biological functionality of modified SF scaffolds for the formation of new bone.

Mimicry is an attractive approach which is used to design materials in many applications, for instance in structural and mechanical engineering [11] and in pharmaceutical [12] and biomedical technologies [13]. In tissue regeneration in particular mimicry is used to create functional scaffolds to enhance new tissue formation. In the case of bone tissue engineering, mimicked scaffolds are designed to have a similar structure and functionality to native extracellular matrix (ECM) [14]. Furthermore, some scaffolds are modified with mimicked functionality by growth factors, to induce new bone formation. Due to this attractive performance, mimicry was chosen as the

approach for preparing the SF scaffolds in this research.

The microenvironment comprises a myriad of biological signals which have been used to induce tissue regeneration [7]. The microenvironment is combined with biocompatible polymers before their fabrication into scaffolds [5, 15]. Due to this unique functionality, the focus in this study was on the microenvironment needed modify the biological functions of the SF scaffolds.

Decellularized tissue is used as an alternative scaffold to induce new tissue formation [14]. Generally, decellularized tissue contains the important microenvironmental components, namely ECM and cytokines [16, 17]. Those components function as signals to induce new tissue formation [18]. Some research has reported the use of decellularized pulp tissue to modify SF scaffolds [19, 20]. That research demonstrated that decellularized pulp tissue could enhance the biological functions of SF scaffolds. Therefore, this research also focused on using decellularized pulp tissue to modify the SF scaffolds.

Fibronectin is a biomolecule that contains various domains. These domains are recognized as regions for cell adhesion that lead to the induction of regeneration of new tissue [21, 22]. Furthermore, they can connect with other biological signals in the microenvironment [20, 23, 24]. Fibronectin is also able to inhibit the inflammatory response during new tissue formation. This study therefore used fibronectin to modify the SF scaffolds.

Our previous study demonstrated that the mimicked environment of fibronectin/decellularized pulp tissue promoted regeneration of bone tissue *in vitro*. The combination of SF scaffolds and fibronectin/decellularized pulp stimulated cell functions such as cell adhesion and proliferation better than SF scaffolds with only decellularized pulp or fibronectin [25]. Based on those results, a combination of fibronectin and decellularized pulp was selected to modify SF scaffolds for *in vivo* testing.

In this research, the SF was fabricated into porous scaffolds before modification by a mimicked microenvironment of fibronectin/decellularized pulp tissue. The modified SF scaffolds were selected and considered for induction of new tissue formation in maxillofacial bone surgery. The *in vivo* testing evaluated the biological performance, morphology and histology of new bone formation.

Materials and methods

Preparation of coated silk fibroin scaffolds

Bombyx mori SF was supplied by the Queen Sirikit Sericulture Centre, Narathiwat, Thailand. We prepared SF scaffolds according to our previous study [25]. The silk solution was concentrated at 3% (w/v). The three-dimensional (3D) SF scaffolds were prepared in five

steps. First, the SF solution was prepared in 48-well plates. Second, it was freeze-dried to make it porous. Third, the porous silk scaffolds were treated by immersion in 70% (v/v) methanol for 30 min. Fourth, the porous silk scaffolds were freeze-dried again. Finally, all SF scaffolds were cut into disks (10 mm in diameter and 2 mm thick).

The primary teeth of children were collected after extraction, which was approved by the Research Ethics Committee (no. MOE 0521.1.03/486). The dental pulp tissue was digested into a solution by collagenase and dispersed for 1 h. The solution was filtered to obtain the decellularized pulp and a freeze-drying machine was used to sublimate the water.

Before coating the SF scaffolds, the decellularized pulp powder was dissolved in 0.1% sodium hypochlorite to a concentration of 0.1 mg ml⁻¹. The solution of fibronectin (bovine plasma, Sigma Aldrich, USA) and decellularized pulp was prepared in a sterile aqueous solution at a 50:50 ratio. The SF scaffolds were soaked in the coating solution for 4 h. The modified SF scaffolds with the ECM-mimicking microenvironment of fibronectin/decellularized pulp (SF-FP) were 10 mm in diameter and 2 mm thick.

Observation by scanning electron microscopy (SEM)

The scaffolds of each group were chosen randomly for observation and evaluation of their morphology, such as pore size and porosity. Gold was used to coat the surfaces of the samples for SEM observation using a gold sputter-coating machine (SPI Supplies, Division of Structure Probe Inc., Westchester, PA, USA). The pore sizes and porosity percentages of the SF and SF-FP scaffolds ($n = 25$) were analyzed by ImageJ software (Wayne Rasband).

Surgical procedure

Twelve male New Zealand white rabbits with a weight of 2.7 ± 0.22 kg (mean \pm standard deviation (SD); range 2.5–3.0 kg) were used. Approval was given by the Animal Ethics Committee (no. MOE 0521.11/520). All surgical procedures were performed under general anesthesia and aseptic conditions by the same surgical team. A 3 cm mid-sagittal incision was made and subperiosteal dissection was carried out to show calvarial bone. A sterilized 10 mm aluminum template was used to ensure that the defects in each animal were the same size. Two 10 mm diameter bicortical defects were cut at the left and right parietal bones. The defects were grafted randomly with the experimental SF-FP and SF scaffolds. The wounds were sutured layer by layer. A single dose of pethidine (10 mg kg⁻¹) was administered intramuscularly for anesthesia. Penicillin G (50 000–100 000 U kg⁻¹) was injected intramuscularly once daily for 3 days and the wound was dressed once a day during three postoperative days. The rabbits were followed closely. Any clinical

changes, such as swelling, color, inflammation, wound dehiscence or tissue necrosis, were recorded. The rabbits were sacrificed 2, 4 and 8 weeks after operation. The calvarium of each rabbit was removed in one block and then immediately immersed in 10% formalin for at least 1 week for tissue fixation before being evaluated by micro-computed tomography (micro-CT) and histology.

Evaluation of new bone formation by micro-CT

All calvarial specimens were scanned by a micro-CT system (μ CT 35 system, Scanco Medical, Bassersdorf, Switzerland) with built-in software. The specimens were scanned perpendicularly to the cranium vault at 70 kVp, 113 μ A and 8 W in high-resolution mode (18.5 $\mu\text{m}^3/\text{voxel}$). The volume of interest was defined to indicate the region of interest and the size of the region. The scanned data reconstructed the 3D (volume of interest) images of the defects. The regions of interest were analyzed using the following parameters: percentage of bone volume by total defect volume (% BV/TV), trabecular thickness (mm) and bone mineral density (mgHA cm^{-3}).

Histology

All calvarial specimens were fixed by 10% formalin for 3 weeks followed by decalcification in 10% ethylenediaminetetraacetic acid (EDTA) pH 7.4 for 4 weeks. They were then dehydrated in a graded ethanol series solutions and xylene, embedded in paraffin, and cut into three sections, each with a thickness of 5 μm . The sections were stained with hematoxylin and eosin. They were examined by a light microscope to evaluate new bone formation, inflammatory response and vascularization.

Statistical analysis

The numerical data are presented as percentage and mean \pm SD, using the Mann–Whitney test to find the differences between the experimental groups at each postoperative time point (2, 4 and 8 weeks). A p -value < 0.05 was considered to be statistically significantly different. All data were analyzed by SPSS (Statistical Package for the Social Sciences, IBM, USA) version 16.0.

Results

Morphological structure of coated SF scaffolds

The SF and SF-FP scaffolds were fabricated into 3D disks (10 mm in diameter and 2 mm thick). The SF-FP scaffolds were slightly brighter than the SF scaffolds. The SF-FP and SF scaffolds were soft, dry and very porous. In figure 1, the SF scaffold is thin and has smooth walls and an interconnecting porous structure (figures 1(a), (b)). On the other hand, the SF-FP scaffold has smaller interconnecting pores and thicker walls than the SF scaffold (figure 1(c)). There were

small fibrils in the pores and small crystal particles which adhered to the surfaces of the walls of the SF-FP scaffold (figure 1(d)). The mean pore sizes of the SF scaffolds and the SF-FP scaffolds were $162.0114 \pm 10.01 \mu\text{m}$ and $109.3659 \pm 10.21 \mu\text{m}$, respectively. The pore sizes were significantly different ($p < 0.001$). However, the percentage porosities were very similar at 85.32% of the SF scaffold, and 83.39% of the SF-FP scaffold.

Gross tissue observation

All rabbits remained alive throughout the experimental period. All wounds demonstrated excellent healing by normal hair growth without any evidence of infection or wound dehiscence. At the time of sacrifice the pericranium tissue of the calvaria had healed without any infection. Macroscopic observation showed that all specimens had excellent healing and there was no evidence of infection. All materials were intimately incorporated with the surrounding host calvarial bone (figure 2). The endocranium also showed good healing at the grafting sites at all time points. The underlying brain and dura layers were intact. However, the SF implants swelled more than the SF-FP implants at 2 weeks (figure 2(d)). The defects of the SF-FP and SF scaffolds were firm at the periphery and rubbery in the middle. Their color was as same as the host bone (figures 2(e), (f)). Importantly, the results showed that both the SF and SF-FP scaffolds exhibited good healing of the bone defects.

Characterization of new bone formation by micro-CT

In 3D reconstruction, the defects which were grafted with the SF scaffolds induced new bone at the periphery of the defect at each postoperative time point (figures 3(a)–(c)). The SF-FP scaffolds induced the formation of new bone at the periphery at 2 and 4 weeks (figures 3(d), (e)) and they enhanced new bone toward the center of the defects at 8 weeks (figure 3(f)).

The percentage of new bone volume fraction of the SF group was lower than the SF-FP group at 2 weeks ($4.34 \pm 2.79\%$ versus $6.89 \pm 1.45\%$, respectively). At 4 weeks, both SF and SF-FP groups increased about 1.5 times ($5.60 \pm 3.40\%$ and $9.52 \pm 1.42\%$, respectively). However, 8 weeks postoperatively all of them were slightly reduced (figure 4(a)). Besides that, the trabecular structure of the SF-FP group was thicker than for the SF group. These thickness increased at 4 weeks and slightly decreased at 8 weeks. There was a significant difference between them at 4 weeks ($p = 0.043$) (figure 4(b)). Bone mineralization in both groups increased from 2 weeks to 4 weeks, and then decreased at 8 weeks. The mineralization of the SF-FP group was higher than in the SF group at all postoperative time points (figure 4(c)).

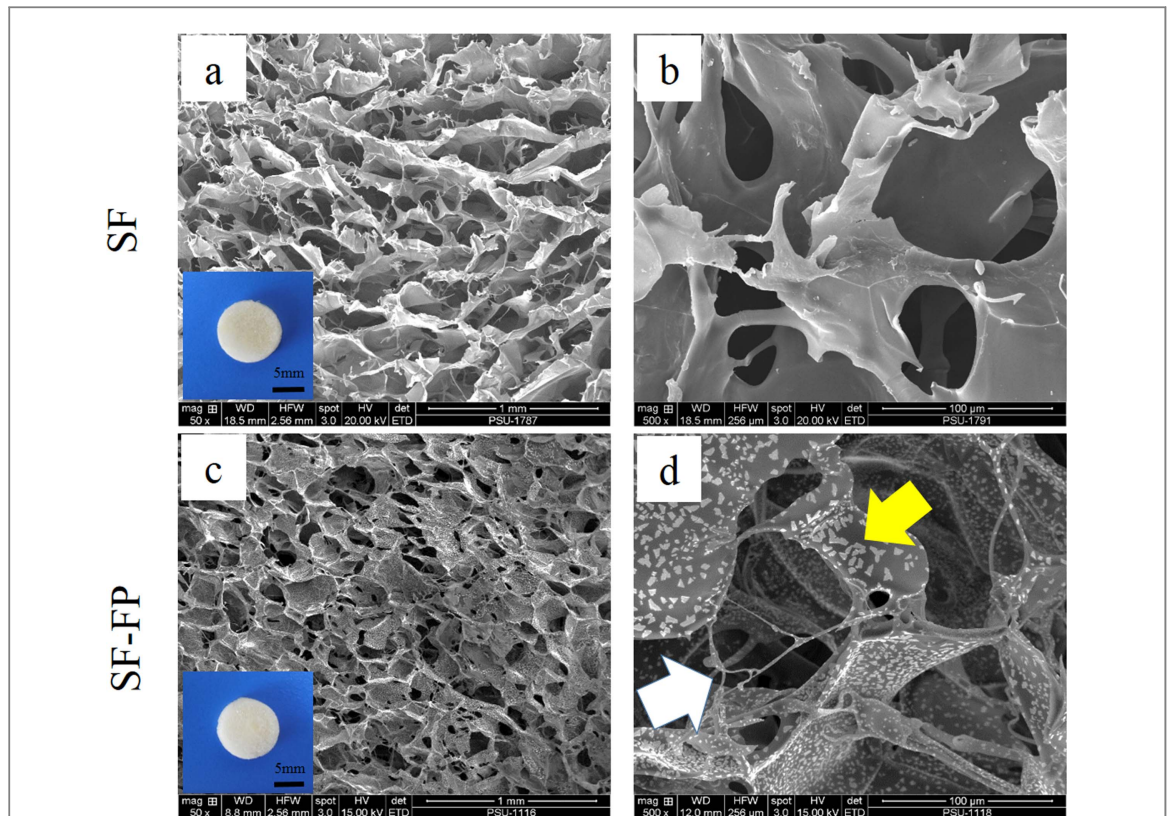


Figure 1. Morphological surfaces of the scaffolds scanned by SEM at $50\times$ (a, c) and $500\times$ (b, d) magnification. The SF scaffold (a, b) is porous with thin, smooth walls, having an interconnecting porous structure. The SF-FP scaffold (c, d) had smaller interconnecting pores and thicker walls. In (d) the fibril structure at an inner pore is indicated by the white arrow and the crystal particles attached to the SF-FP walls by the yellow arrow.

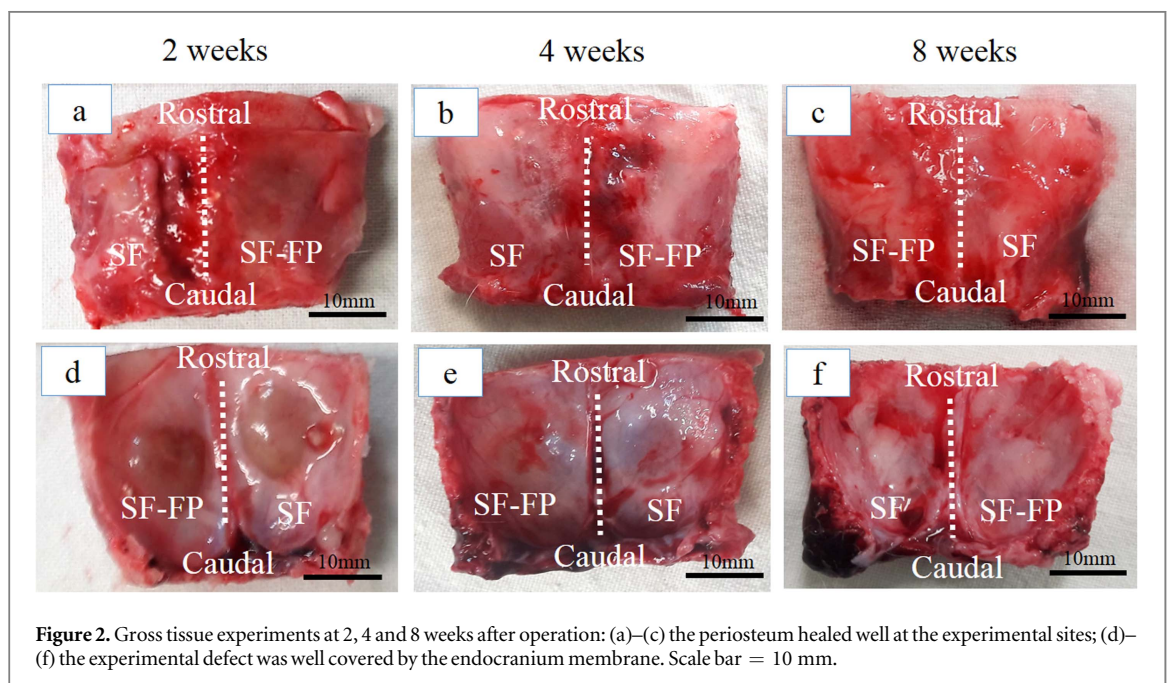
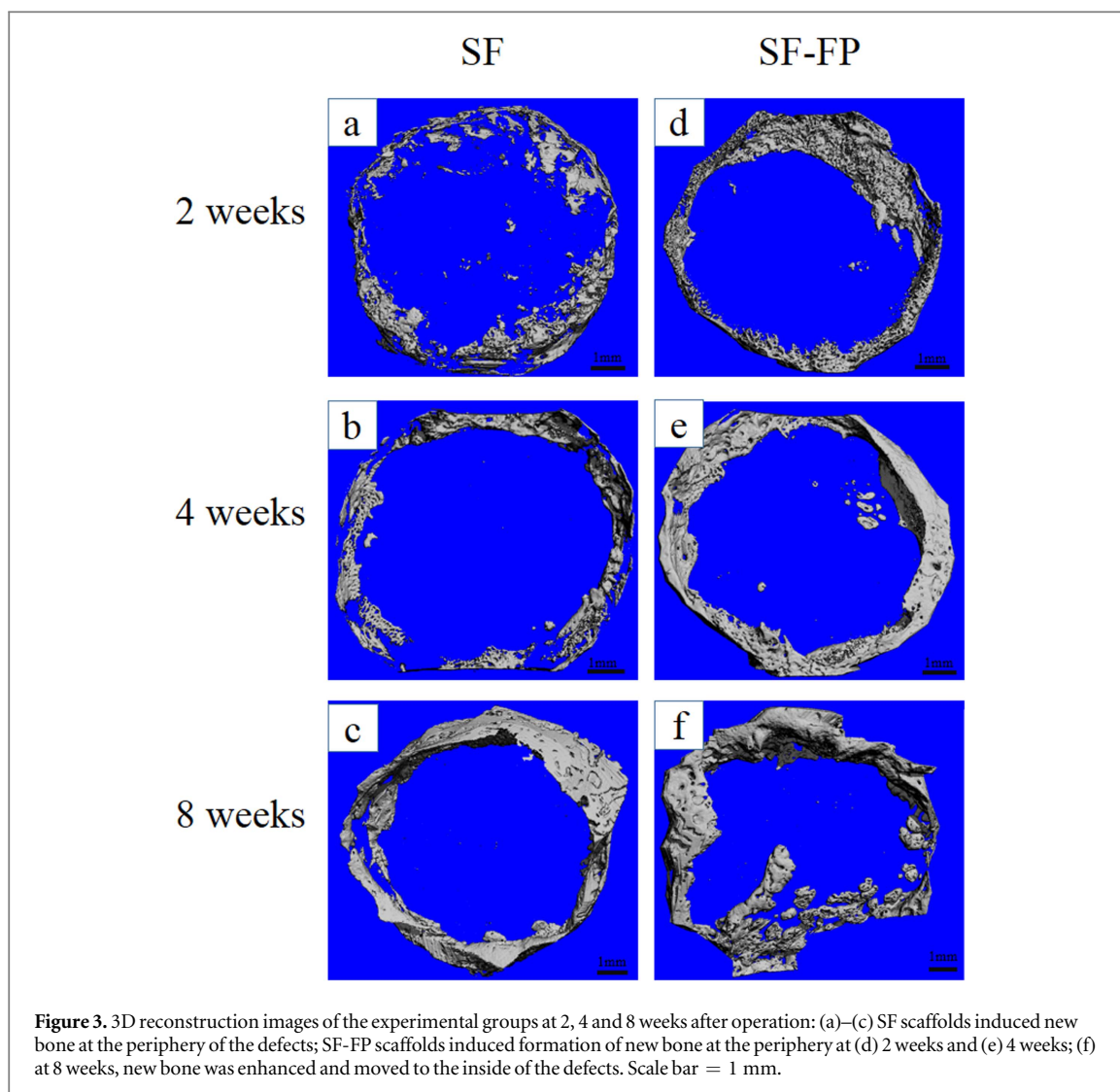


Figure 2. Gross tissue experiments at 2, 4 and 8 weeks after operation: (a)–(c) the periosteum healed well at the experimental sites; (d)–(f) the experimental defect was well covered by the endocranium membrane. Scale bar = 10 mm.

Histology

In figure 5, macroscopic evaluation of the SF scaffold shows the formation of new bone at the periphery and the defect is filled by an inflammatory response such as swelling and a homogeneous purple color due to inflammatory cells at 2 weeks (figure 5(a)). At 4 weeks,

new bone formation in the SF group is enhanced at the periphery, but the SF implant has collapsed in the middle (figure 5(b)). At 8 weeks, new bone formed is immature at the periphery, and fibrous tissue is replaced in the middle (figure 5(c)).



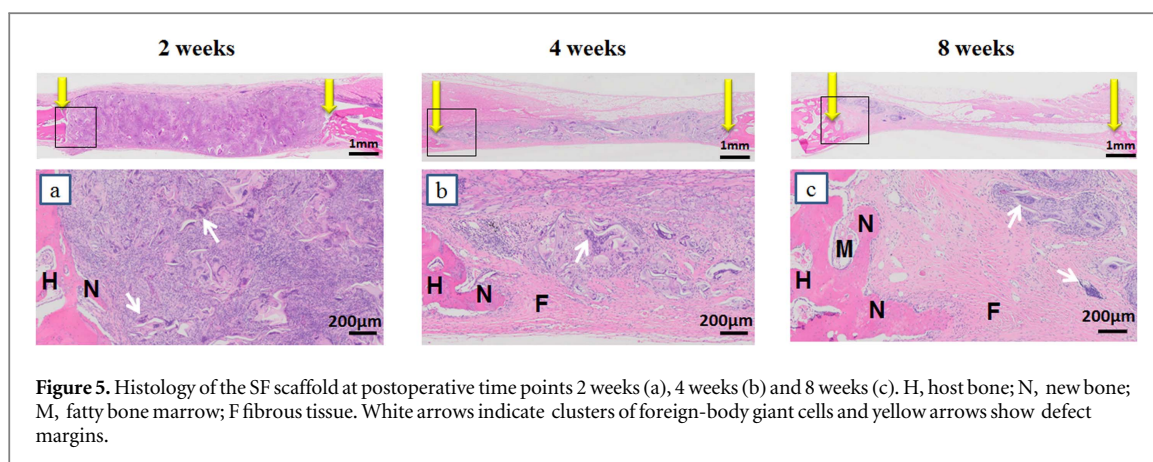
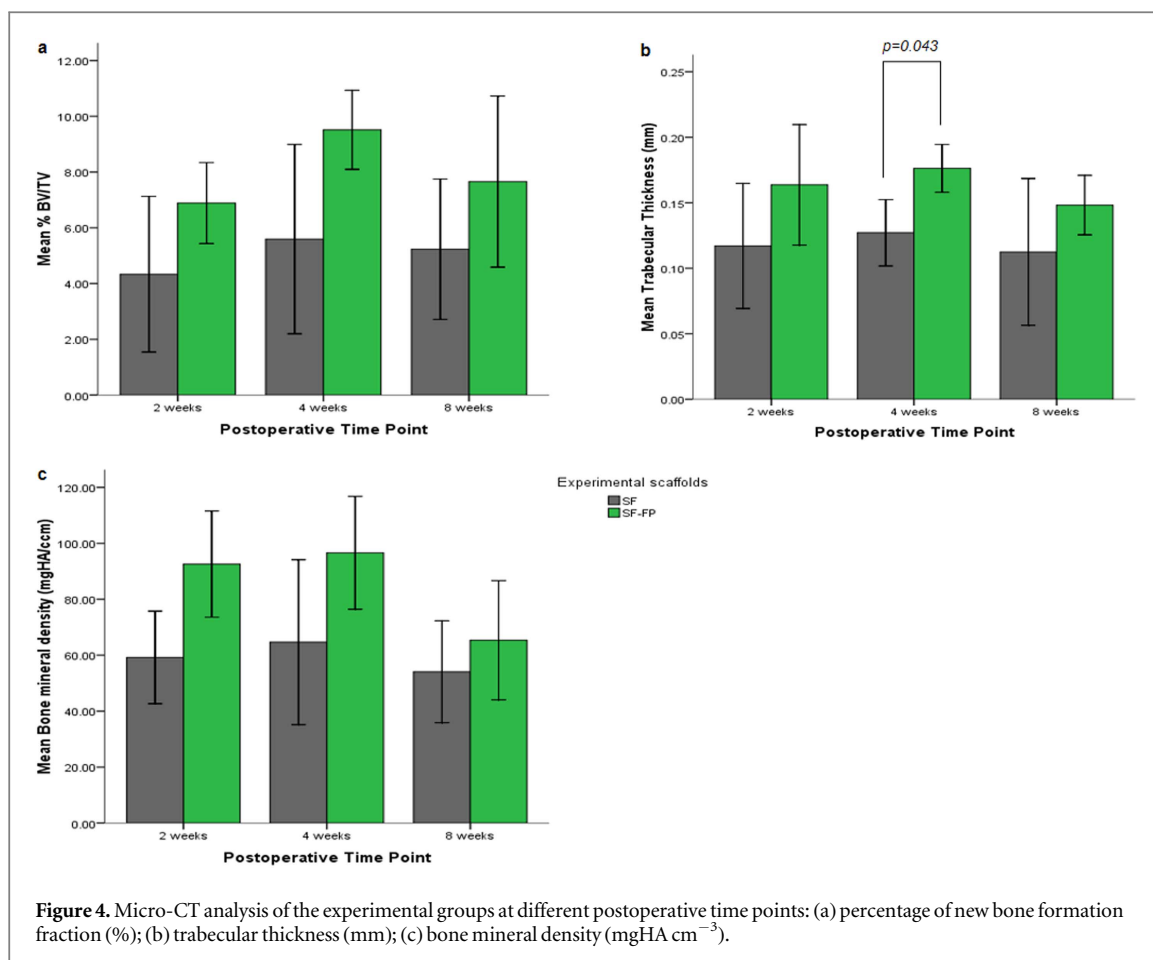
Macroscopic observation in the SF-FP group at 2 weeks indicated that there was no swelling due to an inflammatory response as in the SF group. Vessels and new bone formation were enhanced within the scaffold at the periphery (figure 6(a)). At 4 weeks, the normal size of the scaffold was maintained. New bone formation was enhanced further than the peripheral margins (figure 6(b)). At 8 weeks, the SF-FP scaffold collapsed in the middle as in the SF group. The new bone formed mature fatty bone marrow within the newly formed bone (figure 6(c)).

In figure 7 it can be seen that the SF scaffold clearly triggered clusters of foreign-body giant cells and inflammatory cells, and there was little vascularization within the scaffold at 2 weeks (figure 7(a)). At 4 weeks, the foreign-body reaction decreased and the SF scaffold did not enhance bone formation or vascularization within it (figure 7(b)). At 8 weeks, fibrous tissue was filled the defect and immature bone formed at the periphery of the SF scaffold (figure 7(c)). On the other hand, the SF-FP scaffold had better compatibility than the SF scaffold. It enhanced new bone formation (detected within the residual SF-FP scaffold at the

periphery). Blood vessels and a few foreign-body giant cells were present (figure 7(d)). At 4 weeks, the vascularization of the SF-FP scaffold was better than at 2 weeks. New bone formation was enhanced further than the peripheral margin and a small amount of residual scaffold was present inside the newly formed bone (figure 7(e)). Furthermore, at 8 weeks the mature bone formed was lamellar in the SF-FP group (figure 7(f)).

Discussion

One of the purposes of tissue engineering is the ability to design a proper scaffold to serve as a tissue structure [2]. The purpose of this study was to assess modified SF scaffolds coated with a mimicked microenvironment of fibronectin/decellularized pulp for their biocompatibility and enhancement of new bone formation. Notably, SF-FP had a smaller pore size to SF. That smaller size came from the self-organization of decellularized pulp and fibronectin which adhered in the pores [25]. The scaffolds (10 mm in diameter and 2 mm thick) were implanted bilaterally in rabbit



calvarial defects to demonstrate these properties. All rabbits were observed for clinical healing before their calvaria were harvested at 2, 4 and 8 weeks after operation. The scaffolds were evaluated macroscopically and were observed histologically for the formation of new bone, inflammatory response and vascularization, and the defects were characterized by micro-CT.

The empty control defects were not included in this study because they were filled by fibrous tissue within experimental time points, as in our previous study [26]. Moreover, the modified SF scaffolds with only decellularized pulp or fibronectin did not show

satisfactory results for use in bone regeneration compared with the modified SF scaffolds with a mimicked microenvironment of fibronectin/decellularized pulp in *in vitro* testing [25]. Therefore, these measures helped to cut down the number of animals needed but still satisfied the requirements for statistical analysis [9].

None of the scaffolds showed infection or wound dehiscence (figure 2). Because SF is a biocompatible material [3, 5] the host showed a lower inflammatory response to the SF-FP scaffolds than the SF scaffolds (figure 7). This study demonstrated that decellularized pulp possessed biocompatibility that could induce

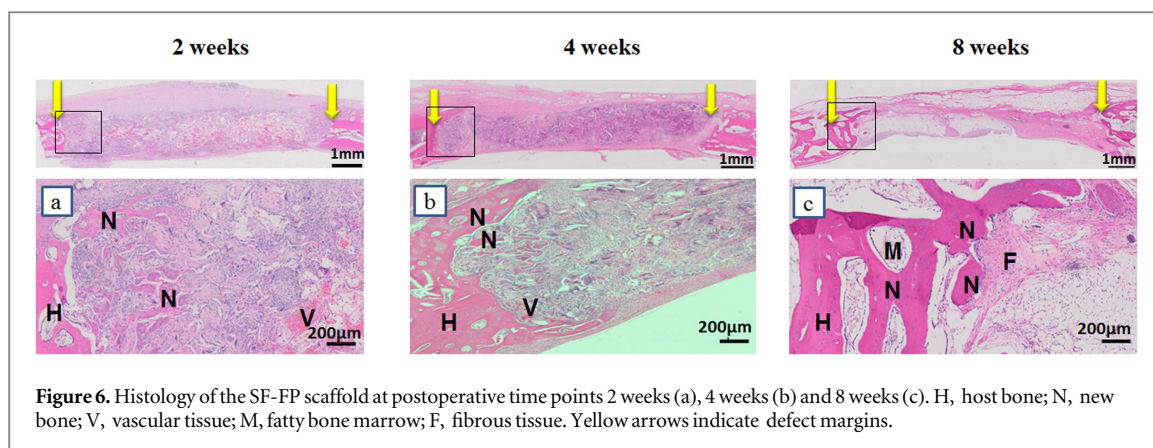


Figure 6. Histology of the SF-FP scaffold at postoperative time points 2 weeks (a), 4 weeks (b) and 8 weeks (c). H, host bone; N, new bone; V, vascular tissue; M, fatty bone marrow; F, fibrous tissue. Yellow arrows indicate defect margins.

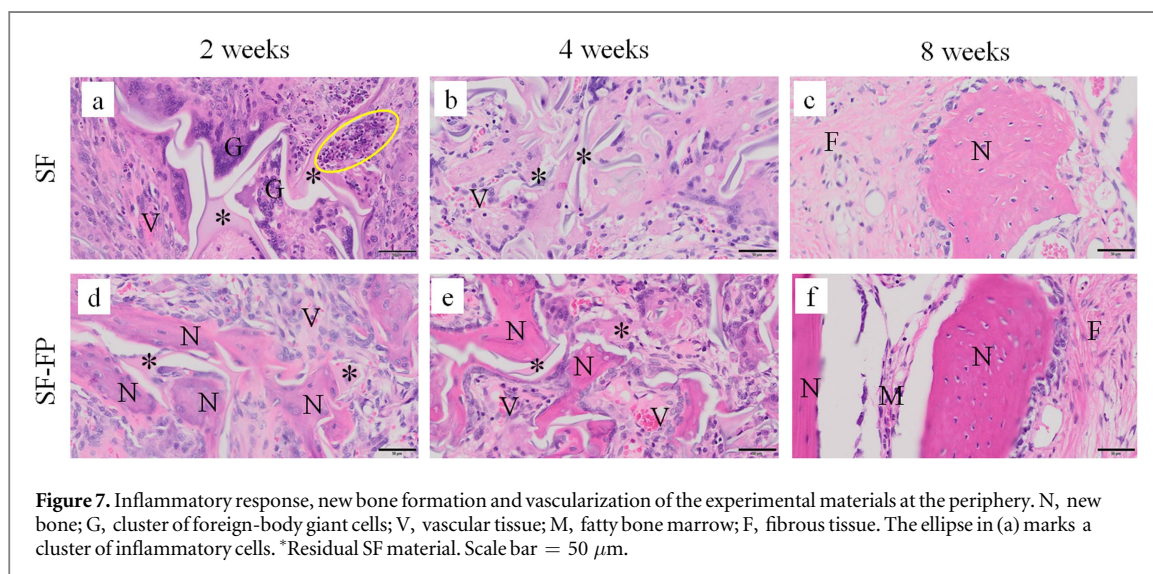


Figure 7. Inflammatory response, new bone formation and vascularization of the experimental materials at the periphery. N, new bone; G, cluster of foreign-body giant cells; V, vascular tissue; M, fatty bone marrow; F, fibrous tissue. The ellipse in (a) marks a cluster of inflammatory cells. *Residual SF material. Scale bar = 50 μm .

osteogenesis [16, 19, 20]. The combination of SF scaffolds with fibronectin led to a small inflammatory reaction and fewer foreign-body cells because the fibronectin reduced the inflammatory response [27].

Vascularization in the SF-FP group was enhanced inside the scaffolds (figure 7). The decreased inflammatory response might benefit vascular enhancement within the experimental scaffolds [6, 27]. The decrease in the inflammatory response was due to the presence of the fibronectin [27]. Vascularization is important for the supply of many essential components in bone formation, such as blood cells, oxygen, minerals and growth factors for cell nutrition [12, 28]. Moreover, the decellularized tissue can induce vascularization [17, 29]. In the case of the SF-FP scaffolds, the enhanced vascularization might come from the synergized functionality of fibronectin and decellularized pulp tissue. Therefore, our results indicate that the mimicked microenvironment of fibronectin/decellularized pulp tissue was able to enhance vascularization. This vascularization led to the induction of new bone formation.

In this study, the SF-FP scaffolds enhanced the formation of new bone better than the SF scaffolds (figure 4). Newly formed bone or woven bone was

detected at the peripheral sites where the recruitment of mesenchymal cells was encouraged in the process of intramembranous ossification (figure 6). The osteoconductive properties were promoted by the fibrillar network and crystal particles of the mimicked microenvironment on the SF-FP scaffolds (figure 1). The mimicked microenvironment was due to reconstruction of the decellularized pulp tissue combined with the fibronectin which adhered to the decellularized dental pulp [25]. This reconstruction could promote adhesion and differentiation of osteoblasts for the formation of new bone [23, 30].

The new bone formed on the SF-FP scaffolds was of better quality than that on the SF scaffolds. This might be due to the components of the ECM dental pulp. The method of decellularization does not remove all components of ECM tissue [18]. The remaining components are large amounts of collagen and non-collagenous proteins, such as collagen type I, III and IV, fibronectin, vitronectin, osteopontin, bone sialoprotein, transforming growth factor-1 (TGF-1), TGF-3, bone morphogenetic protein-2 (BMP-2) and insulin-like growth factor-1 (IGF-1) [16, 18, 20, 29]. Those components facilitate osteoblast adhesion and proliferation at the periphery and within the scaffolds.

Moreover, the trabecular structure in the SF-FP group was harder than in the SF group (figure 4(b)). The fibronectin supported the mimicked SF, which is rich in adhesive proteins in the natural original matrix, for adhesion, proliferation and differentiation of the osteogenic cells for better mineralization than most synthetic materials [23, 30, 31]. As a result, bone quality in the SF-FP group was better than in the SF group. At 8 weeks, bone formed in the SF-FP group was more mature than that in the SF group (figure 7(f)). Bone regeneration with SF-FP implants showed faster remodeling than with SF scaffolds.

The SF-FP scaffolds had smaller pore sizes, and were thus more porous, than the SF scaffolds, leading to increasing amount of fibrils among the inter-connecting pores. Previous studies reported that the pore size must be at least 50 μm to permit bone growth into an artificial scaffold and the internal connective porosity was more important for successful anchorage of bone growth than the overall pore diameter [9, 20, 32]. This study also demonstrated that bone regeneration was affected by the morphological characteristics of the scaffolds, such as the mimicked microenvironment, rather than the pore characteristics of the materials [9, 20, 33].

Conclusion

In this study, modified silk fibroin scaffolds were coated by a mimicked microenvironment of fibronectin/decellularized pulp that had a porous structure with small fibrils and crystal particles from the mimicked microenvironment. The results of *in vivo* testing indicated that the silk fibroin scaffolds could enhance the formation of new bone in rabbit calvaria. Furthermore, they demonstrated good biocompatibility (indicated by a low inflammatory response and good vascularization). Finally, this study showed that coated silk fibroin scaffolds with a mimicked microenvironment of fibronectin/decellularized pulp are promising for use in bone regeneration, particularly in maxillofacial surgery.

Acknowledgments

We would like to thank Ms Supaporn Sangkert and Mr Jakchai Jantaramano who helped us in this study.

ORCID iDs

Thanh H Thai  <https://orcid.org/0000-0003-3430-4873>

References

- [1] Garg A K 2004 *Bone Biology, Harvesting, and Grafting for Dental Implants: Rationale and Clinical Applications* (New Malden: Quintessence Publishing Company)
- [2] Salgado A, Coutinho O and Reis R 2004 Bone tissue engineering: state of the art and future trends *Macromol. Biosci.* **4** 743–65
- [3] Altman G et al 2003 Silk-based biomaterials *Biomaterials* **24** 401–16
- [4] Kundu B, Rajkhowa R, Kundu S C and Wang X 2013 Silk fibroin biomaterials for tissue regenerations *Adv. Drug. Deliv. Rev.* **65** 457–70
- [5] Mandal B, Grinberg A, Gil S, Panilaitis B and Kaplan D 2012 High-strength silk protein scaffolds for bone repair *Proc. Natl Acad. Sci. USA* **109** 7699–704
- [6] Hofmann S et al 2013 Remodeling of tissue-engineered bone structures *in vivo Eur. J. Pharm. Biopharm.* **85** 119–29
- [7] Meinel L and Kaplan D L 2012 Silk constructs for delivery of musculoskeletal therapeutics *Adv. Drug. Deliv. Rev.* **64** 1111–22
- [8] Correia C et al 2012 Development of silk-based scaffolds for tissue engineering of bone from human adipose-derived stem cells *Acta Biomater.* **8** 2483–92
- [9] Uebersax L et al 2013 Biocompatibility and osteoconduction of macroporous silk fibroin implants in cortical defects in sheep *Eur. J. Pharm. Biopharm.* **85** 107–18
- [10] Zhang W et al 2011 The use of injectable sonication-induced silk hydrogel for VEGF(165) and BMP-2 delivery for elevation of the maxillary sinus floor *Biomaterials* **32** 9415–24
- [11] Lutolf M P and Hubbell J A 2005 Synthetic biomaterials as instructive extracellular microenvironments for morphogenesis in tissue engineering *Nat. Biotech.* **23** 47–55
- [12] Salvay D M et al 2008 Extracellular matrix protein-coated scaffolds promote the reversal of diabetes after extrahepatic islet transplantation *Transplantation* **85** 1456–64
- [13] Hinderer S, Layland S and Schenke-Layland K 2016 ECM and ECM-like materials—biomaterials for applications in regenerative medicine and cancer therapy *Adv. Drug. Deliv. Rev.* **97** 260–9
- [14] Cheng C W, Solorio L D and Alsberg E 2014 Decellularized tissue and cell-derived extracellular matrices as scaffolds for orthopaedic tissue engineering *Biotechnol. Adv.* **32** 462–84
- [15] Jiang X et al 2009 Mandibular repair in rats with premineralized silk scaffolds and BMP-2-modified bMSCs *Biomaterials* **30** 4522–32
- [16] Traphagen S B et al 2012 Characterization of natural, decellularized and reseeded porcine tooth bud matrices *Biomaterials* **33** 5287–96
- [17] Badylak S F, Taylor D and Uygun K 2011 Whole-organ tissue engineering: decellularization and recellularization of three-dimensional matrix scaffolds *Annu. Rev. Biomed. Eng.* **13** 27–53
- [18] Benders K, Weeren P R V, Badylak S F, Saris D B F, Dhert W J A and Malda J 2013 Extracellular matrix scaffolds for cartilage and bone regeneration *Trends Biotechnol.* **31** 169–76
- [19] Sangkert S, Kamonmattayakul S, Chai W L and Meesane J 2016 A biofunctional-modified silk fibroin scaffold with mimic reconstructed extracellular matrix of decellularized pulp/collagen/fibronectin for bone tissue engineering in alveolar bone resorption *Mater. Lett.* **166** 30–4
- [20] Sangkert S, Meesane J, Kamonmattayakul S and Chai W L 2016 Modified silk fibroin scaffolds with collagen/decellularized pulp for bone tissue engineering in cleft palate: morphological structures and biofunctionalities *Mater. Sci. Eng. C* **58** 1138–49
- [21] Bini E, Foo C W, Huang J, Karageorgiou V, Kitchel B and Kaplan D L 2006 RGD-functionalized bioengineered spider dragline silk biomaterial *Biomacromolecules* **7** 3139–45
- [22] Wohlrab S et al 2012 Cell adhesion and proliferation on RGD-modified recombinant spider silk proteins *Biomaterials* **33** 6650–9
- [23] Garcia A J and Reyes C D 2005 Bio-adhesive surfaces to promote osteoblast differentiation and bone formation *J. Dent. Res.* **84** 407–13
- [24] Kurihara H and Nagamune T 2005 Cell adhesion ability of artificial extracellular matrix proteins containing a long repetitive Arg-Gly-Asp sequence *J. Biosci. Bioeng.* **100** 82–7

- [25] Sangkert S, Kamonmattayakul S, Chai W L and Meesane J 2017 Modified porous scaffolds of silk fibroin with mimicked microenvironment based on decellularized pulp/fibronectin for designed performance biomaterials in maxillofacial bone defect *J. Biomed. Mater. Res. A* **105** 1624–36
- [26] Wongsupa N, Nuntanaranont T, Kamolmattayakul S and Thuaksuban N 2017 Assessment of bone regeneration of a tissue-engineered bone complex using human dental pulp stem cells/poly(epsilon-caprolactone)-biphasic calcium phosphate scaffold constructs in rabbit calvarial defects *J. Mater. Sci., Mater. Med.* **28** 77
- [27] Meinel L *et al* 2005 The inflammatory responses to silk films *in vitro* and *in vivo* *Biomaterials* **26** 147–55
- [28] Kini U and Nandeesh B N 2012 Physiology of bone formation, remodeling, and metabolism *Radionuclide and Hybrid Bone Imaging* ed I Fogelman *et al* (Berlin: Springer) pp 29–57
- [29] Goldberg M and Smith A 2004 Cells and extracellular matrices of dentin and pulp: a biological basis for repair and tissue engineering *Crit. Rev. Oral Biol. Med.* **15** 13–27
- [30] Mavrogenis A F, Dimitriou R, Parvizi J and Babis G C 2009 Biology of implant osseointegration *J. Musculoskel. Neuron. Interact.* **9** 61–71 PMID: 19516081
- [31] Shekaran A and Garcia A J 2011 Extracellular matrix-mimetic adhesive biomaterials for bone repair *J. Biomed. Mater. Res. A* **96** 261–72
- [32] Hollister S 2009 Scaffold design and manufacturing: from concept to clinic *Adv. Mater.* **21** 3330–42
- [33] Kuboyama N *et al* 2013 Silk fibroin-based scaffolds for bone regeneration *J. Biomed. Mater. Res. B* **101** 295–302